

**$m_T$  Dependence of Boson Interferometry in Heavy Ion Collisions at the CERN SPS**

H. Beker,<sup>1,\*</sup> H. Bøggild,<sup>2</sup> J. Boissevain,<sup>3</sup> M. Cherney,<sup>4</sup> J. Dodd,<sup>5</sup> S. Esumi,<sup>6</sup> C. W. Fabjan,<sup>1</sup> D. E. Fields,<sup>3</sup> A. Franz,<sup>1</sup> K. H. Hansen,<sup>2</sup> E. B. Holzer,<sup>1</sup> T. J. Humanic,<sup>12</sup> B. V. Jacak,<sup>3</sup> R. Jayanti,<sup>7,12</sup> H. Kalechofsky,<sup>7,†</sup> T. Kobayashi,<sup>8,‡</sup> R. Kvatadze,<sup>1,§</sup> Y. Y. Lee,<sup>7,||</sup> M. Leltchouk,<sup>5</sup> B. Lörstad,<sup>9</sup> N. Maeda,<sup>6</sup> A. Medvedev,<sup>5</sup> Y. Miake,<sup>11,¶</sup> A. Miyabayashi,<sup>9</sup> M. Murray,<sup>10</sup> S. Nagamiya,<sup>5</sup> S. Nishimura,<sup>6</sup> E. Noteboom,<sup>4</sup> S. U. Pandey,<sup>12</sup> F. Piuze,<sup>1</sup> V. Polychronakos,<sup>11</sup> M. Potekhin,<sup>5</sup> G. Poulard,<sup>1</sup> A. Sakaguchi,<sup>6</sup> M. Sarabura,<sup>3</sup> K. Shigaki,<sup>8,\*\*</sup> J. Simon-Gillo,<sup>3</sup> W. Sondheim,<sup>3</sup> T. Sugitate,<sup>6</sup> J. P. Sullivan,<sup>3</sup> Y. Sumi,<sup>6</sup> H. van Hecke,<sup>3</sup> W. J. Willis,<sup>5</sup> K. Wolf,<sup>10</sup> and N. Xu<sup>3</sup>

(NA44 Collaboration)

<sup>1</sup>CERN, CH-1211 Geneva 23, Switzerland<sup>2</sup>Niels Bohr Institute, DK-2100 Copenhagen, Denmark<sup>3</sup>Los Alamos National Laboratory, Los Alamos, New Mexico 87545<sup>4</sup>Creighton University, Omaha, Nebraska 68178<sup>5</sup>Columbia University, New York, New York 10027<sup>6</sup>Hiroshima University, Higashi-Hiroshima 724, Japan<sup>7</sup>University of Pittsburgh, Pittsburgh, Pennsylvania 15260<sup>8</sup>National Laboratory for High Energy Physics, Tsukuba 305, Japan<sup>9</sup>University of Lund, S-22362 Lund, Sweden<sup>10</sup>Texas A&M University, College Station, Texas 77843<sup>11</sup>Brookhaven National Laboratory, Upton, New York 11973<sup>12</sup>The Ohio State University, Columbus, Ohio 43210

(Received 20 July 1994)

First results of the  $m_T$  dependence of  $\pi^+\pi^+$  and  $K^+K^+$  correlations from S + Pb collisions at 200 GeV/c per nucleon measured by the focusing spectrometer of the NA44 experiment at CERN are presented. Multidimensional fits characterize the pion and kaon emission volume. The pion radius parameter decreases with increasing  $p_T$ . Furthermore, the pion and kaon radii show a common  $1/\sqrt{m_T}$  dependence. This behavior can be interpreted as a result of a strong momentum-position correlation arising from collective flow.

PACS numbers: 25.75.+r

Two-particle intensity interferometry can provide information on the space-time extent of a particle-emitting source when the emitted radiation is at least partially incoherent [1–3]. Correlation measurements with various particles may be particularly helpful in understanding the dynamical evolution of heavy-ion collisions.

In the experimental search for quark-gluon plasma formation, one suggested signature is the extended emission time of mesons from a system undergoing a phase change; this can be measured by one component of the two-particle correlation function [4,5]. Interpretation of these measurements requires study of the effects of the acceptance of the spectrometer and the dynamics of the particles in the final state. Our procedure is to use a detailed event generator simulating the collision and the hadronic interactions [6] to evaluate the correlations in our acceptance with final state dynamics such as expansion, and compare with our data.

The NA44 experiment measured identified single- and two-particle distributions in 200 GeV/c per nucleon S + Pb collisions at midrapidity, with good acceptance for pairs of particles with small momentum difference. The momentum resolution is  $\delta p/p \approx 0.2\%$  and the  $p_T$  range  $0.0 \leq p_T \leq 1.2$  GeV/c. Our high statistics data

permit multidimensional fits, which may be sensitive to collision dynamics [4,5]. A common dependence on  $m_T$  of radius parameters can indicate collective flow [7], as the momentum-position correlations caused by the flow increase with increasing  $p_T$ . NA44 can address this issue by comparing kaons and pions in different  $p_T$  regions. A Gaussian parametrization gives a reasonable fit to the two-particle correlation functions [3], though the distribution may have a more complex shape [8,9].

Higher  $p_T$  pions may decouple from the system earlier in time [8], include fewer pions from resonance decays [10], and consequently show a smaller radius parameter. The RQMD (version 1.08) event generator [6], which simulates heavy ion collisions, predicts that near midrapidity 23% of the pions with  $p_T$  lower than 200 MeV/c come from long lived resonance ( $\omega, \eta, \eta'$ ) decays, but only 8% of pions with  $p_T \approx 500$  MeV/c arise from those resonances. The strength of the correlation, the  $\lambda$  parameter, is expected to increase with  $p_T$  since fewer high- $p_T$  pions come from  $\eta$  and  $\eta'$  decays.

The NA44 focusing spectrometer [11] uses two dipole magnets and three quadrupoles to create a magnified image of the target. The momentum range in this analysis covers a band of  $\pm 20\%$  around the nominal momentum

setting. Two angular settings of the spectrometer with respect to the beam axis are used, 44 and 131 mrad, and referred to as the low- $p_T$  ( $\langle p_T \rangle \approx 150$  MeV/ $c$ ) and the high- $p_T$  ( $\langle p_T \rangle \approx 450$  MeV/ $c$ ) settings, respectively. The time-of-flight start signal is derived from a Cherenkov beam counter with a time resolution of  $\approx 35$  ps [12]. A silicon pad detector gives the charged-particle multiplicity distribution with  $2\pi$  azimuthal acceptance in the range  $1.5 < \eta < 3.3$ .

Three highly segmented scintillator hodoscopes are used for tracking and time of flight ( $\sigma \approx 100$  ps). Two threshold Cherenkov counters provide additional good particle identification. A uranium-scintillator calorimeter distinguishes electrons, hadrons, and muons.

The single-particle acceptance at 131 mrad setting for pions spans  $2.5 < y < 3.2$  and  $0.2 < p_T < 1.4$  GeV/ $c$ . The acceptance at the 44 mrad setting for the pions spans  $3.2 < y < 4.2$  and  $0.0 < p_T < 0.6$  GeV/ $c$  and for the kaons covers  $2.7 < y < 3.3$  and  $0.0 < p_T < 0.7$  GeV/ $c$ . The 131 mrad data sample contains 50 000 and 38 000 reconstructed pion pairs in the horizontal and vertical settings, respectively. The target thickness is 0.5 cm. Events from the 3% of most central collisions, determined by the Si detector, are used. Contamination of  $\pi$  pairs by  $K\pi$  is less than 1%.

The correlation function is

$$C_{\text{raw}}(\vec{k}_1, \vec{k}_2) = \frac{R(\vec{k}_1, \vec{k}_2)}{B(\vec{k}_1, \vec{k}_2)}, \quad (1)$$

where  $\vec{k}_i$  are the particle momenta. The ‘‘real distribution’’  $R(\vec{k}_1, \vec{k}_2)$  is the measured pair distribution as a function of relative momentum. The ‘‘background distribution’’  $B(\vec{k}_1, \vec{k}_2)$  is generated as follows: For each event in the  $R(\vec{k}_1, \vec{k}_2)$  sample, twenty pairs of events are selected randomly. In these pairs, one particle in each event is used to create a new ‘‘event’’ for the  $B(\vec{k}_1, \vec{k}_2)$  distribution. Pairs constructed in the  $B(\vec{k}_1, \vec{k}_2)$  sample are subjected to the same analysis procedure as the pairs from the real sample.

The background spectrum is distorted with respect to the true uncorrelated two-particle spectrum, owing to the effect of the two-particle correlations on the single-particle spectrum, and is iteratively corrected (the correction factor is referred to as  $K_{\text{SPC}}$ ) [13,14]. The data are further corrected for the momentum resolution of the spectrometer and the two-particle acceptance ( $K_{\text{acc}}$ ) [11].

Coulomb interactions are corrected using the Gamow correction ( $K_{\text{Coul}}$ ). Corrections from Coulomb wave function integration [8] tend to increase the extracted parameter by about 5% but do not affect the  $\lambda$  parameter significantly. After corrections the correlation function is given by

$$C(k_1, k_2) = C_{\text{raw}} K_{\text{SPC}} K_{\text{acc}} K_{\text{Coul}}. \quad (2)$$

Coulomb interactions with the residual nuclear system are neglected but should be small for two particles with identical charge-to-mass ratios which experience similar

accelerations in the Coulomb field [15]. No corrections are made for final-state strong interactions, but these are expected to be small [8]. The data are fitted to three different functions

$$C(Q_{\text{inv}}) = A(1 + \lambda e^{-Q_{\text{inv}}^2 R_{\text{inv}}^2}), \quad Q_{\text{inv}} = \sqrt{Q^2 - Q_0^2}, \quad (3)$$

$$C(Q_{R=\tau}) = A(1 + \lambda e^{-Q_{R=\tau}^2 R_{R=\tau}^2}), \quad Q_{R=\tau} = \sqrt{Q^2 + Q_0^2}, \quad (4)$$

and

$$C(Q_{t_0}, Q_{t_s}, Q_l) = A(1 + \lambda e^{-Q_{t_0}^2 R_{t_0}^2 - Q_{t_s}^2 R_{t_s}^2 - Q_l^2 Q_l^2}). \quad (5)$$

One-dimensional fits using the variables  $Q_{R=\tau}$  and  $Q_{\text{inv}}$  allow comparison with other experiments and different particles, and are useful in cases of limited statistics. Unfortunately the extracted parameters are difficult to interpret. Our data permit an analysis in three dimensions, and partially alleviate this difficulty. The momentum difference is resolved into  $Q_l$  parallel and  $Q_t$  perpendicular to the beam direction;  $Q_t$  is further resolved into a component  $Q_{t_0}$  parallel to the pair momentum sum and  $Q_{t_s}$  perpendicular to the sum. Being parallel to the velocities of the particles,  $Q_{t_0}$  is sensitive to the lifetime of the source, whereas  $Q_{t_s}$  is sensitive only to the transverse spatial extent of the source. Thus the parameters  $R_{t_0}$  and  $R_{t_s}$  give measures of the source lifetime and transverse source size, respectively [8]. The data are analyzed in the frame in which the  $z$  component ( $p_z = p_{z_1} + p_{z_2}$ ) of the pair momentum sum is zero, also referred to as the ‘‘longitudinal center-of-mass system (LCMS).’’ This frame relates the lifetime information to  $Q_{t_0}$ , and simplifies the theoretical formulations of the correlation function for longitudinally boost invariant systems. This arises due to the fact that LCMS comoves longitudinally with the center of the emission region for particles of a given longitudinal momentum [16]. The three-dimensional analysis requires simultaneous fitting of data from the horizontal and vertical spectrometer settings, which optimizes our acceptance in  $Q_{t_0}$  and  $Q_{t_s}$ , respectively. The resolution in  $Q_{R=\tau}$ ,  $Q_{t_0}$ , and  $Q_l$  is  $\approx 15$  MeV/ $c$  and is  $\approx 30$  MeV/ $c$  in  $Q_{t_s}$ . The effects of the finite resolution, independent of  $p_T$ , has been deconvoluted by an iterative procedure. Bin sizes of 15 MeV/ $c$  are used, and all bins are included for fitting.

Systematic errors are estimated by varying the analysis conditions, e.g.,  $p_T$  resolution and hodoscope slat cuts, and refitting the data. The systematic errors are comparable to the statistical ones; further details on systematic error analysis are in Ref. [17].

The results from fits to  $Q_{R=\tau}$  and  $Q_{\text{inv}}$  for the horizontal settings are given in Table I [17,18]. Results from 3D fits to  $\pi^+ \pi^+$  data are shown in Table II. Projections onto the three axes are presented in Fig. 1 using 30 MeV/ $c$  cuts on the nonprojected components. The deviation of the

TABLE I. Results [17,18] of Gaussian parametrizations in  $Q_{inv}$  and  $Q_{R=\tau}$ . ( $\langle p_T \rangle$  in MeV/c.)

System ( $\langle p_T \rangle$ )	$\lambda$	$R(R = \tau)$ (fm)	$\chi^2/N_{dof}$
$\pi^+ \pi^+$ ( $\approx 450$ )	$0.52 \pm 0.05$	$2.36 \pm 0.13$	42/30
$\pi^+ \pi^+$ ( $\approx 150$ )	$0.59 \pm 0.03$	$3.90 \pm 0.14$	24/25
$K^+ K^+$ ( $\approx 240$ )	$0.85 \pm 0.06$	$2.69 \pm 0.14$	65/36

System ( $\langle p_T \rangle$ )	$\lambda$	$R_{inv}$ (fm)	$\chi^2/N_{dof}$
$\pi^+ \pi^+$ ( $\approx 450$ )	$0.48 \pm 0.02$	$4.27 \pm 0.23$	27/20
$\pi^+ \pi^+$ ( $\approx 150$ )	$0.56 \pm 0.02$	$5.00 \pm 0.22$	29/25
$K^+ K^+$ ( $\approx 240$ )	$0.92 \pm 0.08$	$3.22 \pm 0.20$	53/31

$\chi^2/N_{dof}$  from unity in the large angle data and the one-dimensional  $K^+ K^+$  data reflects a difference from a perfect Gaussian at low  $Q$ , as seen in Fig. 2 and Ref. [17].

A trend is evident in all three  $R$  parameters. High- $p_T$  pions have smaller  $R$  parameters than low- $p_T$  pions. The  $R$  parameters for low- $p_T$  kaons [17] and high- $p_T$  pions are comparable. No  $p_T$  dependence is seen on the lambda parameter for the pions.

The prediction of a large  $R_{T_0}$  compared to  $R_{T_s}$ , from hadron emission by a mixed plasma-hadron gas phase, is not borne out by the data. We now discuss our observations in the light of two models which both permit the estimation of geometrical source sizes. Within the framework of the first one, RQMD [6], it is also possible to evaluate the influence of resonances and the experimental acceptance on the  $R$  and  $\lambda$  parameters as a function of increasing  $p_T$ . The shape of the  $\pi\pi$  correlation is influenced by the  $\omega(789)$ , its contribution decreasing considerably from low to high  $p_T$  [19,20]. The correlation functions predicted by RQMD for our acceptance, however, do not show an appreciable increase in  $\lambda$ , in agreement with the data. In contrast to the low- $p_T$  pions, only about 4% of the kaons [21] come from resonances with lifetimes that are long compared to the size of the system. Consequently, the kaon  $R$  parameters should be comparable to those of high- $p_T$  pions.

Reasonable agreement of data on high- $p_T$  pions with RQMD is shown in Fig. 2; RQMD and data show similar trends in the  $R$  parameters. Because of the correlations between position and momentum, which indicate a collective expansion, the  $R$  parameters from the correlation function are, in general, smaller than the source position distribution. This is true for any experimental acceptance [21]. The agreement with RQMD parameters at large  $p_T$

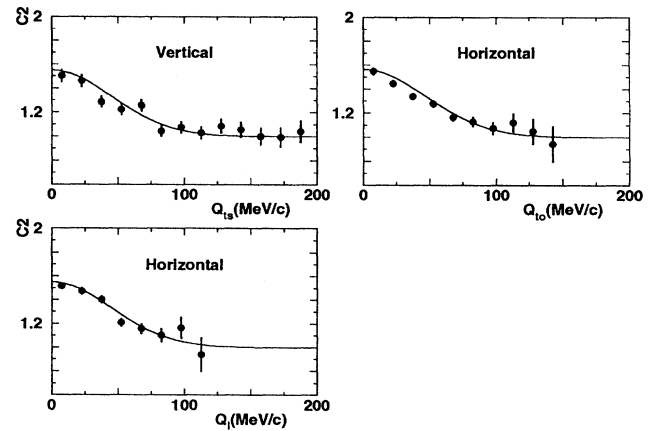


FIG. 1. The  $Q_{T_s}$ ,  $Q_{T_0}$ , and  $Q_l$  projections (131 mrad setting). The lines represent a Gaussian fit to the data points. Error bars are statistical only.

allows us to infer the transverse spatial dimension of the pion source at freeze-out. The  $R_{T_s}$  parameter calculated from RQMD, which most closely reflects the source transverse size, is  $3.25 \pm 0.12$  fm for high- $p_T$  pions, while the width of a Gaussian fit to the transverse position distribution of high- $p_T$  pions at freezeout in the model is 3.5 fm.

We also compare our measurements to a simple hydrodynamical model, which predicts the  $R$  parameters to scale as  $1/\sqrt{m_T}$  [7] for all mesons. The collective expansion leads to strong momentum-position correlations in both longitudinal and transverse directions [22,23]. The velocity gradient together with the freeze-out temperature generate a length scale in all three dimensions. If the source length scales are considerably larger than this, for a cylindrically symmetric three-dimensional expansion, the three measured  $R$  parameters become equal in the LCMS and show a  $1/\sqrt{m_T}$  dependence [7]. Our measurements, summarized in Table III, indicate that, in the LCMS,

$$R_l \approx R_{T_0} \approx R_{T_s} \propto 1/\sqrt{m_T}. \quad (6)$$

This model implies that the source dimensions are larger than the extracted  $R$  parameters from the correlation function.

Both models discussed include a collective expansion, explicitly in the hydrodynamical model, and as a consequence of the rescattering in RQMD. The data indicate the presence of expansion but cannot address the relative validity of the two models.

TABLE II. Results [17,18] of Gaussian parametrizations in  $Q_{T_0}$ ,  $Q_{T_s}$ , and  $Q_l$ . ( $\langle p_T \rangle$  in MeV/c.)

System	$\lambda$	$R_{T_0}$ (fm)	$R_{T_s}$ (fm)	$R_l$ (fm)	$\chi^2/N_{dof}$
$\pi^+ \pi^+$ ( $\approx 450$ )	$0.55 \pm 0.02$	$2.97 \pm 0.16$	$2.95 \pm 0.24$	$3.09 \pm 0.19$	1500/1095
$\pi^+ \pi^+$ ( $\approx 150$ )	$0.56 \pm 0.02$	$4.02 \pm 0.14$	$4.15 \pm 0.27$	$4.73 \pm 0.26$	1201/1415
$K^+ K^+$ ( $\approx 240$ )	$0.82 \pm 0.04$	$2.77 \pm 0.12$	$2.55 \pm 0.20$	$3.02 \pm 0.20$	925/1011

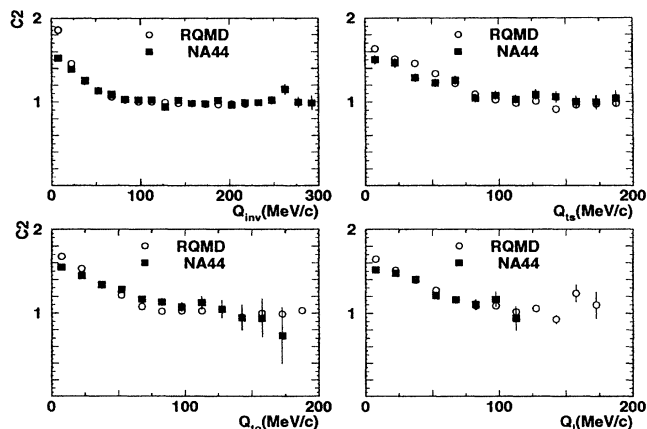


FIG. 2. Comparison of data with RQMD calculation of the correlation function (131 mrad setting).

TABLE III. Results of the  $m_T$  dependence on radius parameter in the LCMS. ( $\langle p_T \rangle$  is in MeV/c,  $m_T$  is in GeV/c, and the  $R$  values are in fm.)

System ( $\langle p_T \rangle$ )	$\sqrt{m_T}$	$\sqrt{m_T} R_{t_0}$	$\sqrt{m_T} R_{t_s}$	$\sqrt{m_T} R_t$
$\pi^+ \pi^+$ ( $\approx 450$ )	0.68	$2.0 \pm 0.1$	$2.0 \pm 0.1$	$2.1 \pm 0.1$
$\pi^+ \pi^+$ ( $\approx 150$ )	0.47	$1.9 \pm 0.1$	$2.0 \pm 0.1$	$2.2 \pm 0.1$
$K^+ K^+$ ( $\approx 240$ )	0.74	$2.1 \pm 0.1$	$1.9 \pm 0.20$	$2.2 \pm 0.2$

We have investigated the  $m_T$  dependence of boson correlation functions in S + Pb collisions. The  $R$  parameters for pions and kaons show a  $1/\sqrt{m_T}$  dependence. This dependence can be explained by the presence of strong position-momentum correlations, arising from collective flow. We intend to further investigate this by careful comparison of hydrodynamical model predictions [7,24] to single particle spectra of  $\pi$ ,  $K$ ,  $p$ , and  $d$ ,  $p$ - $p$  correlations, and  $d/p$  ratios.

The NA44 Collaboration wishes to thank the staff of the CERN PS-SPS and the technical staff of CERN and the collaborating institutes for their valuable contributions. In addition, we would like to thank Scott Pratt and T. Csörgő for their numerous suggestions and advice. We are also grateful for the support given by the Science Research Council of Denmark, the W.M. Keck Foundation, the Japanese Society for the Promotion of Science, and the Ministry of Education, Science, and Culture, Japan, the Österreichische Fond zur Förderung

der wissenschaftlichen Forschung, the Science Research Council of Sweden, the U.S. Department of Energy, and the National Science Foundation.

\*Present address: Rome I Institute, Rome I-00185, Italy.

†Now at University of Geneva, CH-1211 Geneve 4, Switzerland.

‡Now at Riken Linac Laboratory, Riken, Saitama 351-01, Japan.

§Visitor from Tbilisi State University, Tbilisi, Republic of Georgia.

||Now at GSI Laboratory, Darmstadt, Germany.

¶Now at Tsukuba University, Tsukuba 305, Japan.

\*\*Now at University of Tokyo, Tokyo 113, Japan.

- [1] R. Hanbury-Brown and R. Q. Twiss, *Nature (London)* **178**, 1046 (1956).
- [2] M. Gyulassy, S. K. Kauffmann, and L. W. Wilson, *Phys. Rev. C* **20**, 2267 (1979).
- [3] B. Lörstad, *Int. J. Mod. Phys. A* **4**, 2861 (1988).
- [4] S. Pratt, *Phys. Rev. D* **33**, 1314 (1986).
- [5] G. Bertsch and G.E. Brown, *Phys. Rev. C* **40**, 1830 (1989).
- [6] H. Sorge, H. Stöcker, and W. Greiner, *Nucl. Phys.* **A498**, 567c (1989).
- [7] T. Csörgő and B. Lörstad, Report No. LUNFD6/(NFF1-7082) (to be published).
- [8] S. Pratt, T. Csörgő, and J. Zimányi, *Phys. Rev. C* **42**, 2646 (1990).
- [9] R. Lednicky and T.B. Progulova, *Z. Phys. C* **55**, 295 (1992).
- [10] M. Gyulassy and S. Padula, *Phys. Rev. C* **41**, 21 (1990).
- [11] H. Beker *et al.*, *Phys. Lett. B* **302**, 510 (1993).
- [12] N. Maeda *et al.*, *Nucl. Instrum. Methods Phys. Res., Sect. A* **346**, 132 (1994).
- [13] K. Kadija and P. Seyboth, *Phys. Lett. B* **287**, 362 (1992).
- [14] W. A. Zajc *et al.*, *Phys. Rev. C* **29**, 2173 (1984).
- [15] D. Boal, C. Gelbke, and B. Jennings, *Rev. Mod. Phys.* **62**, 553 (1990).
- [16] T. Csörgő and S. Pratt, Report No. KFKI-1991-28/A.
- [17] H. Beker *et al.*, *Z. Phys. C* **64**, 209 (1994).
- [18] H. Bøggild *et al.*, "Directional Dependence of the Pion Source in High-Energy Heavy-Ion Collisions" [*Phys. Lett. B* (to be published)].
- [19] J. Sullivan *et al.*, *Nucl. Phys.* **A566**, 531 (1994).
- [20] J. Bolz *et al.*, *Phys. Rev. D* **47**, 3860 (1993).
- [21] J. Sullivan *et al.*, *Phys. Rev. Lett.* **70**, 3000 (1993).
- [22] B. R. Schlei *et al.*, *Phys. Lett. B* **293**, 275 (1992).
- [23] R. Venugopalan *et al.*, *Nucl. Phys.* **A566**, 473 (1994).
- [24] E. Schnedermann *et al.*, *Phys. Rev. C* **48**, 2462 (1993).